

peak response closer to the visual than the haptic peak, as with MLE integration. If degrading the visual input causes the response distribution of the visual neurons to spread, then multiplication of the visual and haptic distributions yields a peak closer to the haptic peak, again as in MLE integration. Thus, the estimator variances (and therefore the weights) do not have to be calculated explicitly: the behaviour of an MLE integrator might be achieved through interactions among populations of visual and haptic neurons. □

Methods

Stimuli

The stimulus was a horizontal bar raised 30 mm above a plane; the bar and plane were perpendicular to the line of sight (Fig. 2a). The width of the bar was 150 mm; its height varied but the average was $S_0 = 55$ mm. Observers viewed the bar binocularly and/or grasped it with the index finger and thumb in order to estimate its height (Fig. 2a). Its vertical position was varied randomly from trial to trial.

The haptic stimulus was generated using two PHANTOM (SensAble Technologies) force-feedback devices (Fig. 2a), one each for the index finger and thumb. Finger and thumb movements had all six degrees of freedom in the 20-cm³ workspace. The three-dimensional positions of the tips of the finger and thumb were monitored, and appropriate forces were applied when the tips reached the positions of the simulated haptic objects. PHANTOMs compellingly simulate haptic properties such as the size, shape and stiffness of the bar. The apparatus was calibrated to align the visual and haptic stimuli spatially.

The visual stimulus was a random-dot stereogram simulating the background plane and bar (Fig. 2). The dots subtended 8 arcmin at the 50-cm viewing distance. Dot density was roughly 9 dots per degree². New dots were displayed with each presentation. The positions of the finger and thumb (tracked by the PHANTOMs) were indicated by small three-dimensional markers; the markers were visible until the bar was touched. Noise was added to the visual display to vary its reliability. The noise was a random displacement of the dot depths in the stereogram (direction parallel to line of sight). The displacements were drawn from a random uniform distribution whose range was 0, 67, 133 or 200% of the 3-cm depth step between the bar and plane. The displacement of the dots is shown in Fig. 2. No noise was added to the haptic display.

We wanted the presentation times for the visual and haptic stimuli to be identical. In the vision-alone discrimination experiment, the standard and comparison stimuli were displayed for 1 s each. In the haptic-alone discrimination experiment, the haptic stimulus began when the thumb and finger both contacted the bar and ended after 1 s. In the visual-haptic trials, the visually specified bar did not appear until the bar was touched by both fingers simultaneously and the visual and haptic stimuli were extinguished after 1 s.

Procedure

Within-modality discrimination was measured in a two-interval, forced-choice scheme. Each trial consisted of the sequential (visual or haptic) presentation of two bars. In the standard interval, the bar was always 55 mm tall and in the comparison interval, it was shorter or taller than 55 mm. The standard and comparison stimuli were randomly assigned to the first or second interval. The observer indicated the interval containing the apparently taller stimulus. The comparison height was varied according to the method of constant stimuli. We plotted psychometric functions, that is the proportion of trials in which the comparison was perceived as taller than the standard against the comparison height. From these functions, we could determine PSEs and discrimination thresholds. Half of the vision-alone and haptic-alone discrimination experiments were conducted (in random order) before the visual-haptic experiment and the other half were conducted after.

In the visual-haptic experiment, observers were again presented two stimuli sequentially: the standard stimulus (visually and haptically specified heights differed by Δ) and the comparison stimulus (visually and haptically specified heights were the same). The average height of the standard stimulus was always 55 mm and the visual-haptic difference (Δ) ranged from -6 to +6 mm. The height of the comparison varied. The observer indicated the interval containing the apparently taller stimulus. Trials with different conflicts were presented in random order to prevent visomotor adaptation.

No feedback was given in any of the experiments. Four observers (aged 22 to 33), naive to the experimental purpose, participated. They were right handed and had normal or corrected-to-normal vision. The observers were questioned at the end: none of them had noticed the conflicts between the visually and haptically specified heights.

Received 25 July; accepted 15 November 2001.

1. Rock, I. & Victor, J. Vision and touch: An experimentally created conflict between the two senses. *Science* **143**, 594–596 (1964).
2. Hay, J. C., Pick, H. L. Jr & Ikeda, K. Visual capture produced by prism spectacles. *Psychonomic Sci.* **2**, 215–216 (1965).
3. Warren, D. H. & Rossano, M. J. in *The Psychology of Touch* (eds Heller, M. A. & Schiff, W.) 119–137 (Erlbaum, Hillsdale, New Jersey, 1991).
4. Power, R. P. The dominance of touch by vision: Sometimes incomplete. *Perception* **9**, 457–466 (1980).
5. Welch, R. B. & Warren, D. H. Immediate perceptual response to intersensory discrepancy. *Psychol. Bull.* **88**, 638–667 (1980).

6. Lederman, S. J. & Abbott, S. G. Texture perception: Studies of intersensory organization using a discrepancy paradigm, and visual versus tactual psychophysics. *J. Exp. Psychol. Hum. Percept. Perform.* **7**, 902–915 (1981).
7. Heller, M. A. Haptic dominance in form perception with blurred vision. *Perception* **12**, 607–613 (1983).
8. Clark, J. J. & Yuille, A. L. *Data Fusion for Sensory Information Processing Systems* (Kluwer Academic, Boston, 1990).
9. Blake, A., Bülthoff, H. H. & Sheinberg, D. Shape from texture: Ideal observer and human psychophysics. *Vision Res.* **33**, 1723–1737 (1993).
10. Landy, M. S., Maloney, L. T., Johnston, E. B. & Young, M. Measurement and modeling of depth cue combination: In defense of weak fusion. *Vision Res.* **35**, 389–412 (1995).
11. Gharamani, Z., Wolpert, D. M. & Jordan, M. I. in *Self-organization, Computational Maps, and Motor Control* (eds Morasso, P. G. & Sanguineti, V.) 117–147 (Elsevier, Amsterdam, 1997).
12. Knill, D. C. Discrimination of planar surface slant from texture: Human and ideal observers compared. *Vision Res.* **38**, 1683–1697 (1998).
13. Backus, B. T. & Banks, M. S. Estimator reliability and distance scaling in stereoscopic slant perception. *Perception* **28**, 417–442 (1999).
14. van Beers, R. J., Sittig, A. C. & Denier van der Gon, J. J. Integration of proprioceptive and visual position information: An experimentally supported model. *J. Neurophysiol.* **81**, 1355–1364 (1999).
15. Schrater, P. R. & Kersten, D. How optimal depth cue integration depends on the task. *Int. J. Comp. Vis.* **40**, 71–89 (2000).
16. Gibson, J. J. Adaptation, after-effect, and contrast in the perception of curved lines. *J. Exp. Psychol.* **16**, 1–31 (1933).
17. Festinger, L., Burnham, C. A., Ono, H. & Bamber, D. Efference and the conscious experience of perception. *J. Exp. Psychol.* **74** (4), 1–36 (1967).
18. Singer, G. & Day, R. H. Visual capture of haptically judged depth. *Percept. Psychophys.* **5**, 315–316 (1969).
19. Tastevin, J. En partant de l'expérience d'Aristote. *L'Encephale* **1**, 57–84 (1937).
20. Mon-Williams, M., Wann, J. P., Jenkinson, M. & Rushton, K. Synaesthesia in the normal limb. *Proc. R. Soc. Lond. B* **264**, 1007–1010 (1997).
21. Pavani, F., Spence, C. & Driver, J. Visual capture of touch: out-of-the-body experiences with rubber gloves. *Psycholog. Sci.* **11**, 353–359 (2000).
22. Heller, M. A. Visual and tactual texture perception: Intersensory cooperation. *Percept. Psychophys.* **31**, 339–344 (1982).
23. Banks, M. S. & Backus, B. T. Extra-retinal and perspective cues cause the small range of the induced effect. *Vision Res.* **38**, 187–194 (1998).
24. Ernst, M. O., Banks, M. S. & Bülthoff, H. H. Touch can change visual slant perception. *Nature Neurosci.* **3**, 69–73 (2000).
25. Peña, J. L. & Konishi, M. Auditory spatial receptive fields created by multiplication. *Science* **292**, 249–252 (2001).

Acknowledgements

We thank M. Landy for comments on the manuscript; and H. Ernst, X. Moncada, C. Alderson and S. Kashiwada for participating as observers. This research was supported by research grants from Air Force Office of Scientific Research and the National Institutes of Health, and by an equipment grant from Silicon Graphics.

Competing interests statement

The authors declare that they have no competing financial interests.

Correspondence and requests for materials should be addressed to M.O.E. (e-mail: marc.ernst@tuebingen.mpg.de).

Effects of grouping in contextual modulation

Michael H. Herzog* & Manfred Fahle*†

* Human Neurobiology, University of Bremen, Argonnenstrasse 3, 28211 Bremen, Germany

† City University, Department of Optometry and Visual Science, Tait Building, Northampton Square, London EC1V 0HB, UK

Perception of a visual target and the responses of cortical neurons can be strongly influenced by a context surrounding the target^{1–27}. This observation relates to the fundamental issue of how cortical neurons code objects of the external world. In high-contrast regimes, embedding a target in an iso-oriented context reduces neural responses and deteriorates performance in psychophysical experiments. Performance from orthogonal surrounds is better than that from iso-oriented ones^{1–17}. This contextual interference is often postulated to be caused by long- or short-range interac-

tions between neurons tuned to orientation. Here we show, using a new illusion called 'shine-through' as a sensitive psychophysical probe, that the orientation difference between target and context does not determine performance. Instead, contextual modulation depends on the overall spatial structure of the context. We propose that contextual suppression vanishes if the contextual elements are grouped to an independent and coherent object.

In the shine-through illusion^{4,5}, a briefly displayed vernier precedes a grating referred to as the 'standard grating', which comprises more than seven aligned elements (see Fig. 1). Subjectively, the vernier shines through the grating and appears brighter, wider, longer and superimposed on the grating. Vernier discrimination thresholds can be as small as 20 arcsec, whereas those for an unmasked vernier can be around 8 arcsec, indicating a masking effect of the grating. Homogeneity of the standard grating is a prerequisite for the effect to occur; even very subtle spatial deviations from this homogeneity markedly diminish the shine-through effect^{4,5}.

Four iso-oriented contextual elements markedly degrade performance (that is, the thresholds of offset discrimination increase; Fig. 2a, g). This finding agrees with most studies using high-contrast target regimes¹⁻¹⁸. Performance improves, however, if more iso-oriented contextual elements are displayed. For 25 contextual lines, performance is about the same as that for the standard grating, and significantly better than that for a display with 4 contextual elements (Fig. 2a, b). Horizontal contextual lines yield analogous results: performance improves if small horizontal elements become part of a long horizontal line (Fig. 2c, d). One line on both sides of the standard grating (Fig. 2e) yields significantly lower performance than two lines placed on only one side (Fig. 2f). Thus, the overall spatial structure rather than the orientation difference between target and context determines contextual suppression.

Both a decrease (Fig. 2f) and an increase (Fig. 2b) of the number of contextual lines improve performance compared with four contextual lines; therefore, the number of lines is neither necessary nor sufficient to predict performance. A better explanation is that contextual suppression vanishes if the elements of the context are grouped to a coherent object.

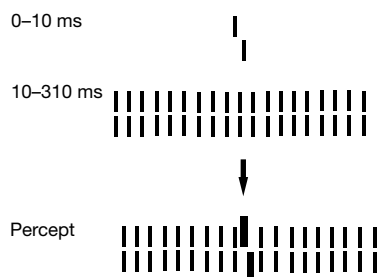


Figure 1 The shine-through effect. A vernier, consisting of two abutting lines, presented for a short time (10–30 ms) shines through a following grating if the grating comprises more than seven elements. The shine-through element appears to be wider, brighter and even longer than the preceding vernier really is. This grating is called the 'standard grating'. With less than seven grating elements the vernier remains invisible to the observer^{4,5}. Except for offset, all spatial parameters of grating elements were the same as those of the preceding vernier. The horizontal spacing between grating elements was 200 arcsec, and verniers were 1,260 arcsec long presented for the shortest duration at which shine-through just occurred. Stimuli were displayed on an analog monitor (HP 1334A) controlled by a Power Macintosh computer through fast 16-bit digital-to-analog converters (pixel rate 1 MHz). Luminance was about 80 cd m⁻². Subjects were asked to discriminate the offset direction (left versus right) of the shine-through element by pressing one of two push buttons. Incorrect responses were followed by an error signal produced by the computer. Thresholds were determined with an adaptive staircase method (the offset size of the vernier yielding 75% correct responses). Statistical analysis was performed on logarithmic data. See ref. 5.

The contextual gratings shown in Fig. 3a, which do not diminish shine through, strongly degrade performance if attached to the standard grating (Fig. 3b). Attaching these gratings creates an inhomogeneous central grating; therefore, vernier discrimination decreases (see ref. 5). Only a minor spatial change has occurred because the vertical gap between the contextual and the standard grating is only 200 arcsec wide; in other words, it is much smaller than the receptive fields of most cortical neurons. Moreover, the overall intensity of the whole context is identical. Thus, it seems to matter strongly whether the context is an independent part of the visual display (ref. 6, but see refs 15, 17).

Contextual interference emerges in a fast dynamic process. We presented single contextual verniers preceding two contextual gratings and a vernier preceding the central standard grating (Fig. 4b). The contextual verniers appear as distinct shine-through elements, whereas the visibility of the central target vernier is strongly diminished; therefore, vernier discrimination deteriorates markedly (Fig. 4e) compared to the condition of Fig. 4a. Arrays of more than one contextual vernier do not, in general, shine through a following

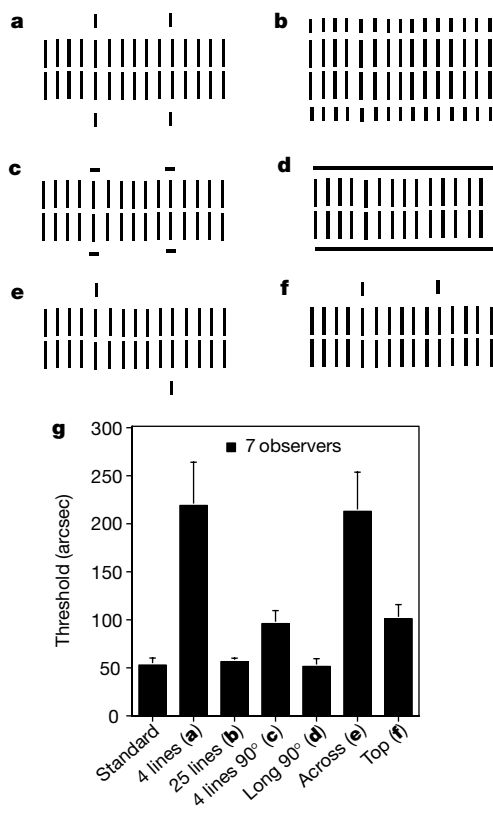


Figure 2 Contextual interference cannot be predicted by contextual orientation. A vernier (not shown) preceded a grating with 25 elements (15 are shown) flanked by contextual lines presented simultaneously with the grating. The vertical gap between contextual lines and grating was 200 arcsec. **a**, Four vertical lines of 400 arcsec length were displayed above and below the third grating element on both sides. **b**, Twenty-five contextual elements appeared above and below the standard grating. **c**, Four lines were oriented orthogonal to the grating (that is, horizontal). **d**, Two long horizontal lines flanked the whole grating. **e**, Two lines were displayed, one above left and the other below right of middle. **f**, Only two lines above the grating were displayed. **g**, Performance for 4 contextual lines is lower, hence thresholds are higher, than that for 25 elements, even though these 4 lines are part of the 25 contextual lines (paired *t*-test, $P = 0.0024$). For some observers, the shine-through element is completely invisible for four contextual lines and vernier discrimination thresholds cannot be determined (a threshold of 350 arcsec is recorded in these cases). Four small horizontal lines interfere more strongly than two long horizontal lines (paired *t*-test, $P = 0.0105$). If two lines are arranged on one side of the grating, performance is better than if elements are in corresponding positions on different sides of the grating (paired *t*-test, $P = 0.005$).

grating. Thus, three aligned contextual verniers, each preceding contextual gratings, remain invisible (Fig. 4c). Even so, the arrays of contextual verniers inhibit the single central vernier, which therefore remains largely invisible. Offset discrimination of this vernier deteriorates strongly—comparable to the condition with single contextual verniers. Thus, suppression by preceding contextual verniers is not caused by the subjective visibility of the preceding contextual elements themselves.

A vernier and a grating three times longer than standard (Fig. 4d), mimicking an attachment of contextual verniers and gratings to the central standard vernier and grating, improve performance significantly compared with the separated gratings and verniers shown in Fig. 4b. Attachment here leads to temporal and spatial homogeneity in contrast to the conditions in Fig. 3, where spatial inhomogeneities of the standard grating degrade performance. Again, contextual intensity is identical for stimuli in Fig. 4b and d, whereas thresholds are not.

Contextual suppression diminishes if the suppressive contextual elements of Fig. 2a are presented without a following grating (data not shown). Therefore, it is the backward masking nature of the shine-through effect that reveals contextual modulation during the first milliseconds of cortical information processing^{10,15,28}.

In most psychophysical and physiological studies using high-contrast targets, contextual suppression is strongest for iso-oriented contexts and decreases for orthogonal ones^{1–17}. For example, responses of a neuron to a line presented in its receptive field strongly decrease when several iso-oriented contextual lines appear in the surrounding non-classical receptive field^{1–3}. Neural responses increase if the number of these contextual lines decreases (ref. 1, but see ref. 2). The underlying neural mechanisms are thought to rely on orientation-specific horizontal connections or on high-level back projections. For low-contrast targets a more complex pattern occurs, revealing facilitating effects in addition^{8,16,19–23}.

Contextual surrounds are homogeneous in most studies. We compared various contextual layouts and thus could evaluate context–context modulation in addition to context–target modulation. Contrary to the above results, we found that increasing the number of iso-oriented contextual elements improves performance (see Fig. 2a, b). An extended iso-oriented, homogeneous surround and a long, orthogonal (that is, horizontal) contextual line yield performance comparable to that of the standard condition (that is, the standard grating without any surround). Clearly, commonly

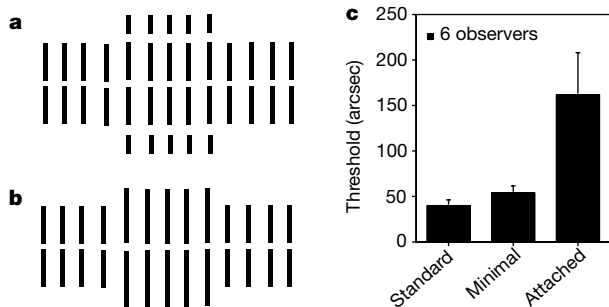


Figure 3 Independence of the context matters. **a**, We determined the minimal number of iso-oriented contextual elements for which interference is absent so that fewer elements would yield a deterioration of performance. For four observers this number was five lines, whereas for two subjects it was seven (only 13 elements of the standard grating are shown). The vertical gap between contextual lines and standard grating was 200 arcsec. **b**, Contextual gratings were directly attached to the standard grating; that is, the gap between contextual and standard gratings was removed. **c**, Performance strongly deteriorates if gratings that cause almost no contextual interference ('minimal') are attached to the central grating ('attached'; paired *t*-test, $P = 0.0085$). Note that the minimal gratings contain the four contextual elements from the condition in Fig. 2a. Vertical bars symbolize standard errors of the means of all six paid student observers.

used low-level descriptions such as orientation, number, and overall intensity of contextual elements are not sufficient to explain the results.

We propose that the overall spatial structure of the context, rather than its individual low-level features, determines modulation. A context does not interfere if it can be grouped to a coherent and independent gestalt—in other words, if the context is an independent entity and all its elements are bound together, or if unbound parts are remote from the target.

Although the influence of contextual elements seems to be complex if based on a low-level stimulus description, the neural mechanism underlying contextual grouping may be simple^{8–10,29}. For example, to explain the shine-through effect, a model has been proposed on the basis of a single neural layer with lateral interactions whose dynamics are described by a partial differential equation (C. W. Eurich, U. Ernst and M.H.H., unpublished data; see also ref. 29). According to this equation, neural activity representing the inner elements of a grating decreases compared with that at the edges. For small gratings, this enhanced activity corresponding to the edges suppresses the neural activity corresponding to the

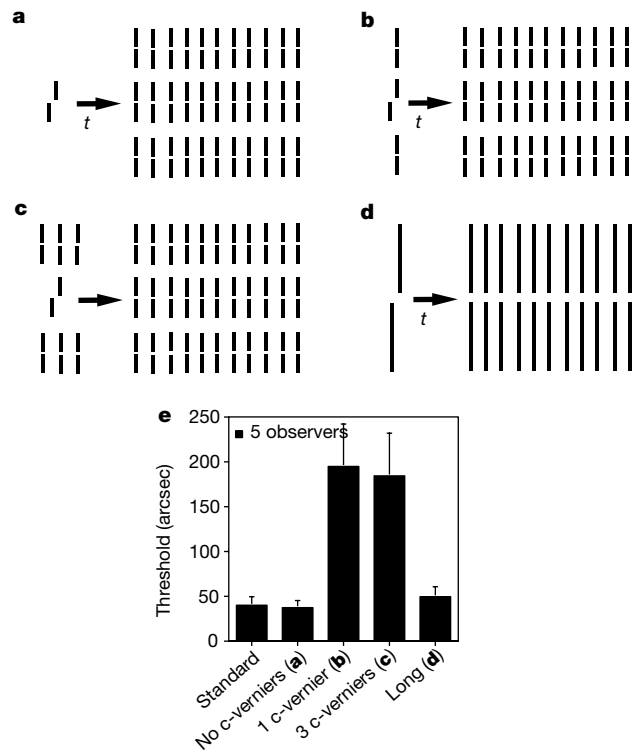


Figure 4 Shine through interferes with shine through. Here, time (*t*) proceeds from left to right rather than from top to bottom. Preceding verniers always appeared at the central position of the corresponding gratings. The standard condition was applied first (see Fig. 1). **a**, As in the condition with 25 contextual elements (Fig. 2b), a vernier preceded the standard grating that was flanked above and below by two identical copies of itself. **b**, As in **a**, except that the contextual gratings were each preceded by a straight vernier, and an offset vernier preceded the standard grating. **c**, Three aligned verniers preceded each of the contextual gratings, an offset one preceded the standard grating. **d**, The grating and vernier were three times longer than in the standard condition. This stimulus had the same energy as in condition **b** and almost the same size. **e**, The standard and the condition in **a** yield comparable performance levels, reaffirming that contextual energy *per se* is not important. Performance in **b** is greatly impaired compared with that in **a** (paired *t*-test, $P = 0.0053$); the contextual verniers (c-verniers), although visible themselves, seriously impair the visibility and therefore offset discrimination for the central vernier. The condition in **c** shows the same impairment as in **b**. Here, the triple verniers, although not visible, impair the discriminability of the central vernier. Contextual interference vanishes when the separated contextual gratings are replaced by a lengthening of the standard grating and vernier (paired *t*-test, $P = 0.0081$ for **c** versus **d**).

vernier. For the same reason, activity corresponding to four isolated (that is, unbound) contextual elements (Fig. 2a) might not be decreased by neighbouring contextual elements and, thus, might produce high neural activity inhibiting the vernier target. For the extended standard grating, shine through is possible because little neural activity occurs in the vernier's close neighbourhood. Analogously, extended contextual gratings might not interfere with the vernier because activity corresponding to their inner elements is weak. Therefore, context–context inhibition prevents context–target suppression of the vernier target.

Contextual elements might directly influence the firing pattern of cortical neurons that code the vernier. For example, the activity of a neuron that is responding vigorously to a vernier target should diminish when isolated contextual elements are presented together with the standard grating. By contrast, increasing the number of contextual elements should yield a rebound of activity. Because vernier display times are short, we expect strongest modulation effects in the transient response of the neurons—that is, in the activity immediately after the presentation of the target. □

Received 17 July; accepted 20 November 2001.

1. Knierim, J. J. & van Essen, D. C. Neuronal responses to static texture patterns in area V1 of the alert macaque monkey. *J. Neurophys.* **67**, 961–980 (1992).
2. Li, W., Thier, P. & Wehrhahn, C. Contextual influence on orientation discrimination of humans and responses of neurons in V1 of alert monkeys. *J. Neurophys.* **83**, 941–954 (2000).
3. Nothdurft, H.-C., Gallant, J. L. & van Essen, D. C. Response modulation by texture surround in primate area V1: Correlates of pop-out under anesthesia. *Vis. Neurosci.* **16**, 15–34 (1999).
4. Herzog, M. H. & Koch, C. Seeing properties of an invisible element: feature inheritance and shine-through. *Proc. Natl Acad. Sci. USA* **98**, 4271–4275 (2001).
5. Herzog, M. H., Fahle, M. & Koch, C. Spatial aspects of object formation revealed by a new illusion, shine-through. *Vis. Res.* **41**, 2325–2335 (2001).
6. Mareschal, I., Sceniak, M. P. & Shapley, M. Contextual influences on orientation discrimination: binding local and global cues. *Vis. Res.* **41**, 1915–1930 (2001).
7. Wehrhahn, C., Li, W. & Westheimer, G. Patterns that impair discrimination of orientation in human vision. *Perception* **25**, 1053–1064 (1996).
8. Stemmler, M., Usher, M. & Niebur, E. Lateral interactions in primary visual cortex: a model bridging physiology and psychophysics. *Science* **269**, 1877–1880 (1995).
9. Li, Z. Contextual influences in V1 as a basis for pop out and asymmetry in visual search. *Proc. Natl Acad. Sci. USA* **96**, 10530–10535 (1999).
10. Wolfson, S. S. & Landy, M. S. Long range interactions between oriented texture elements. *Vis. Res.* **39**, 933–945 (1999).
11. Nothdurft, H. C. Texture segmentation and pop-out from orientation contrast. *Vis. Res.* **31**, 1073–1078 (1991).
12. Cannon, M. W. & Fullenkamp, S. C. Spatial interactions in apparent contrast: inhibitory effects among grating patterns of different spatial frequencies, spatial positions and orientations. *Vis. Res.* **31**, 1985–1998 (1991).
13. Lamme, V. A. The neurophysiology of figure-ground segregation in primary visual cortex. *J. Neurosci.* **15**, 1605–1615 (1995).
14. Zipser, K., Lamme, V. A. F. & Schiller, P. H. Contextual modulation in primary visual cortex. *J. Neurosci.* **16**, 7376–7389 (1996).
15. Caputo, G. The role of the background: Texture segregation and figure-ground segmentation. *Vis. Res.* **36**, 2815–2826 (1996).
16. Sengpiel, F., Sen, A. & Blakemore, C. Characteristics of surround inhibition in cat area 17. *Exp. Brain Res.* **116**, 216–228 (1997).
17. Sillito, A. M., Grieve, K. L., Jones, H. E., Cudeiro, J. & Davis, J. Visual cortical mechanisms detecting focal orientation discontinuities. *Nature* **378**, 492–496 (1995).
18. Macknik, S. L. & Livingstone, M. S. Neuronal correlates of visibility and invisibility in the primate visual system. *Nature Neurosci.* **1**, 144–149 (1998).
19. Polat, U. & Sagi, D. Lateral interactions between spatial channels: suppression and facilitation revealed by lateral masking experiments. *Vis. Res.* **33**, 993–999 (1993).
20. Kapadia, M. K., Ito, M., Gilbert, C. D. & Westheimer, G. Improvement in visual sensitivity by changes in local context: parallel studies in human observers and in V1 of alert monkeys. *Neuron* **15**, 843–856 (1995).
21. Levitt, J. B. & Lund, J. S. Contrast dependence of contextual effects in primate visual cortex. *Nature* **387**, 73–76 (1997).
22. Bonneh, Y. & Sagi, D. Effects of spatial configuration on contrast detection. *Vis. Res.* **38**, 3541–3543 (1998).
23. Yu, C. & Levi, D. Surround modulation in human vision unmasked by masking experiments. *Nature Neurosci.* **3**, 724–728 (2000).
24. Das, A. & Gilbert, C. D. Topography of contextual modulations mediated by short-range interactions in primary visual cortex. *Nature* **399**, 655–661 (1999).
25. Chubb, C., Sperling, G. & Solomon, J. A. Texture interactions determine perceived contrast. *Proc. Natl Acad. Sci. USA* **86**, 9631–9635 (1989).
26. Weisstein, N. & Harris, C. S. Visual detection of lines segments: an object-superiority effect. *Science* **186**, 752–755 (1974).
27. Banks, W. P. & White, H. Lateral interference and perceptual grouping in visual detection. *Percept. Psychophys.* **36**, 285–295 (1984).
28. Kurylo, D. D. Time course of perceptual grouping. *Percept. Psychophys.* **59**, 142–147 (1997).
29. Ernst, U. A., Pawelzik, K. R., Sahar-Pikielny, C. & Tsodyks, M. V. Intracortical origin of visual maps. *Nature Neurosci.* **4**, 431–436 (2001).

Acknowledgements

This work was supported by the Center of Excellence (SFB) ‘Neurocognition’ of the German Research Council (Deutsche Forschungsgemeinschaft). We thank M. Repnow for technical support; and B. Gillam, C. Eurich, U. Ernst, A. Etzold, B. Zenger, K. Neumann, F. Kandil, J. Solomon, M. Morgan, J. Zanker and U. Schmonsees for discussions.

Competing interests statement

The authors declare that they have no competing financial interests.

Correspondence and requests for materials should be addressed to M.H.H. (e-mail: mherzog@uni-bremen.de).

Prediction of central nervous system embryonal tumour outcome based on gene expression

Scott L. Pomeroy*, Pablo Tamayo†, Michelle Gaasenbeek‡, Lisa M. Sturla*, Michael Angelo†, Margaret E. McLaughlin‡, John Y. H. Kim*§, Liliana C. Goumnerova||, Peter M. Black||, Ching Lau¶, Jeffrey C. Allen#, David Zagzag*, James M. Olson***, Tom Curran††, Cynthia Wetmore††, Jaclyn A. Biegel‡‡, Tomaso Poggio§§, Shayan Mukherjee§§, Ryan Rifkin§§, Andrea Califano|||, Gustavo Stolovitzky|||, David N. Louis¶¶, Jill P. Mesirov†, Eric S. Lander††† & Todd R. Golub†††

* Division of Neuroscience, Department of Neurology; † Department of Pathology; ‡ Department of Neurosurgery; § Department of Medicine, Children’s Hospital; ¶ Department of Pediatric Oncology, Dana-Farber Cancer Institute; and ¶¶ Department of Pathology and Neurosurgical Service, Massachusetts General Hospital, Harvard Medical School, Boston, Massachusetts 02115, USA
 † Whitehead Institute/MIT Center for Genome Research, and §§ McGovern Institute, Center for Biological and Computational Learning, AI Lab, Massachusetts Institute of Technology, Cambridge, Massachusetts 02139, USA
 ¶ Division of Pediatric Oncology, Baylor College of Medicine, Houston, Texas 77030, USA
 # Beth Israel Medical Center, New York 10128, USA
 ** Department of Pathology, New York University School of Medicine, New York 10016, USA
 *** Clinical Research Division, Fred Hutchinson Cancer Research Center, Seattle, Washington 98109, USA
 †† Department of Developmental Neurobiology, St Jude Children’s Research Hospital, Memphis, Tennessee 38105, USA
 ‡‡ Division of Human Genetics, The Children’s Hospital of Philadelphia, Department of Pediatrics, University of Pennsylvania School of Medicine, Philadelphia, Pennsylvania 19104, USA
 §§ Department of Biology, Massachusetts Institute of Technology, Cambridge, Massachusetts 02139, USA
 ||| IBM Watson Research Center, Yorktown Heights, New York 10598, USA

Embryonal tumours of the central nervous system (CNS) represent a heterogeneous group of tumours about which little is known biologically, and whose diagnosis, on the basis of morphologic appearance alone, is controversial. Medulloblastomas, for example, are the most common malignant brain tumour of childhood, but their pathogenesis is unknown, their relationship to other embryonal CNS tumours is debated^{1,2}, and patients’ response to therapy is difficult to predict³. We approached these problems by developing a classification system based on DNA microarray gene expression data derived from 99 patient samples. Here we demonstrate that medulloblastomas are molecularly distinct from other brain tumours including primitive neuroectodermal tumours (PNETs), atypical teratoid/rhabdoid tumours